ELSEVIER

Inorganica Chimica Acta 275–276 (1998) 340–348

Inorganica Chimica Acta

Synthesis, X-ray structure and bonding of tris(2,2-6,6-tetramethylheptane-3,5-dionato) bismuth(III)

L. Armelao [a], G. Bandoli [b], M. Casarin [c], G. Depaoli [c], E. Tondello [a,c,*], A. Vittadini [a]

[a] *Centro SRCC del CNR, via Marzolo 1, I-35131 Padua, Italy*

[b] *Dipartimento di Scienze Farmaceutiche, Università di Padova, via Marzolo 5, I-35131 Padua, Italy*

[c] *Dipartimento di Chimica Inorganica, Metallorganica ed Analitica, Università di Padova, via Loredan 4, I-35131 Padua, Italy*

Received 1 July 1997; received in revised form 2 September 1997; accepted 26 September 1997

Abstract

The title compound $[Bi(dpm)_3]$ has been synthesized and its molecular structure determined by single-crystal X-ray diffraction. Two different crystalline forms have been found: $[(Bi(dpm)_3]\cdot H_2O$ (**1**) and $[(Bi(dpm)_3]\cdot 3H_2O$ (**2**). **1** crystallizes in the space group $P2_1/n$ with $a=12.426(5)$, $b=19.565(11)$, $c=15.820(9)$ Å, $\beta=94.31(4)°$, $V=3835(2)$ Å^3, $Z=4$. **2** crystallizes in the space group *Pbcn* with $a=20.953(5)$, $b=19.619(6)$, $c=19.475(3)$ Å, $V=8006(3)$ Å^3, $Z=8$. The coordination around the Bi atom consists of a distorted pentagonal pyramid with two ligands approximately lying in the basal plane while the third one is in a vertical mirror plane. Molecules are associated in dimer units because of the presence of weak interactions in the crystal lattices. The bonding of the monomer compound has been investigated by means of quasi-relativistic quantum-mechanical calculations on the simpler acetylacetonate complex. The metal–ligand interaction is found to be dominated by ionic interactions with a significant repulsion between the Bi 6s lone pair and the symmetric n_+ ligand based combination of the oxygen lone pairs. Such electronic repulsion is reduced, but not eliminated, by relativistic effects. Optimized geometrical parameters obtained by carrying out calculations in the C_s symmetry point group are in good agreement with experiment. Interestingly, however, the pseudo-octahedral D_3 structure is found to be lower in energy, suggesting that the observed pyramidal molecular structure cannot be explained on the basis of simple stereochemical arguments.

Keywords: Crystal structures; Bonding complexes; Bismuth complexes; Diketonate complexes

1. Introduction

Bismuth(III) oxides are interesting materials for various technological applications ranging from heterogeneous catalysis to the production of superconductor and photorefractive materials [1]. High-quality Bi_2O_3 thin films can be grown in principle by chemical vapor deposition or sol–gel techniques, provided that molecular precursors are available. So far, suitable bismuth(III) compounds remain rather limited, and, consequently, Bi_2O_3-based materials have mostly been obtained by traditional high-temperature solid-state reactions. Bismuth(III) β-diketonates have been recently proposed as sources of oxide precursors, but very little is still known about them. A few studies have appeared in literature [2], reporting about the preparation and characterization of $Bi(R^1COCHCOR^2)_3$ where (a) $R^1=R^2=CF_3$; (b) $R^1=CF_3CF_2CF_2$; $R^2=CMe_3$; (c) $R^1=CF_3$; $R^2=CMe_3$; (d) $R^1=R^2=CMe_3$; (e) $R^1=R^2=CMe_3$.

Bi(III) is characterized by the presence of the 6s lone pair. The valence-shell electron-pair repulsion (VSEPR) [3] theory suggests for exacoordinate trivalent complexes of the heavier group 16 elements (As, Sb and Bi) a distorted octahedral coordination. In complexes with bidentate ligands this implies a distortion from a D_3 to either a C_s or a C_3 symmetry [4,5]. However, the stereoactivity of the s lone pair in Sb and Bi compounds is still not well assessed [6]. In this respect, first-principle quantum mechanical calculations can be very helpful.

2. Experimental

2.1. Synthesis and characterization

Tris(2,2-6,6-tetramethylheptane-3,5-dionato) bismuth(III) $[Bi(dpm)_3]$ was prepared starting from $Bi(C_6H_5)_3$ (Aldrich) and dpmH ($(CH_3)_3$–CCOCH$_2$COC–$(CH_3)_3$) (Aldrich) by the following reaction [2]:

$$Bi(C_6H_5)_3 + 3dpmH \rightarrow Bi(dpm)_3 + 3C_6H_6$$

* Corresponding author. Tel: +39 49 827 5227; fax: +39 49 827 5227.

0020-1693/98/$19.00
PII S0020-1693(97)06105-7

The synthesis was carried out in a two-neck flask equipped with a Vigreux column and a water condenser. An excess of dpmH (50%) was used, and a nitrogen flux was maintained in order to drive off the benzene produced in the reaction. The starting system, consisting of the white solid $Bi(C_6H_5)_3$ and the colorless liquid β-diketone, turned to a bright yellow solution upon raising the temperature to 180°C. A period of 6 h was required to transform approximately 50% of the starting compound. The bismuth(III) β-diketonate was finally sublimed under reduced pressure (5×10^{-2} Torr) at 120°C. The product appeared as a white crystalline solid. Since $Bi(dpm)_3$ hydrolyzes very rapidly, all manipulations were carried out in a glove box ($O_2<10$ ppm, $H_2O<2$ ppm). Diffuse reflectance FT-IR spectra were recorded on a Brucker IFS66 spectrometer. ^1H and ^{13}C NMR spectra were recorded in $CDCl_3$ on a JEOL FX90Q. All characterization data were in good agreement with those reported in literature [2].

$Bi(dpm)_3$ crystals suitable for X-ray data collection were obtained by cooling benzene solutions from RT to −4°C, and they were found to be in two different crystalline forms: **1** and **2**. Crystals were handled in a dry-box and sealed in a glass capillary before introduction into the diffractometer.

2.2. X-ray crystallography

Data were collected on colorless transparent parallelepipeds on a Siemens Nicolet R3m/V four-circle automated diffractometer. Owing to the relatively small amount of high-angle data and the rapid deterioration of the crystals on X-ray exposure, in the collection the 2θ range was restricted and the scan-speed was raised. The intensities were corrected for crystal deterioration, while an empirical absorption correction was impossible to be performed. Crystallographic data are given in Table 1. The structures were solved by the heavy-atom method and refined by full-matrix procedures, anisotropically only for Bi atoms. The final electron density difference maps were featureless apart from some broad positive peaks in the vicinity of Bi atoms. The SHELXTL-PLUS [7] package of computer programs was employed for the solution and refinement of the structures. Final atomic coordinates and thermal parameters are reported in Table 2, while relevant distances and angles are listed for both complexes in Table 3.

2.3. Computational details

Our calculations have been performed by running the ADF package [8], based on the density functional (DF) theory, and developed by Baerends and coworkers [9]. A triple-zeta Slater-type basis set with a single polarization function was used for all the atoms. For oxygen and carbon, a frozen potential was used for the 1s electrons; for bismuth the electrons up to 5p were frozen.

To reduce the computational effort, the ligands were replaced by simple acetylacetonate (acac) moieties. The

Table 1
Structure determination summary [a]

	1	2
Crystal data		
Empirical formula	$C_{15}H_{17}O_6Bi\cdot H_2O$	$C_{15}H_{17}O_6Bi\cdot 3H_2O$
M	776.45	812.48
Crystal size (mm)	0.1×0.1×0.2	0.2×0.2×0.5
Crystal system	monoclinic	orthorhombic
Space group	$P2_1/n$	$Pbcn$
a (Å)	12.426(5)	20.953(5)
b (Å)	19.565(11)	19.619(6)
c (Å)	15.820(9)	19.475(3)
β (°)	94.31(4)	
U (Å^3)	3835(2)	8006(3)
Z; D_c (Mg m^{-3})	4; 1.344	8; 1.348
μ (mm^{-1})	4.6	4.4
$F(000)$	1584	3328
Data collection		
2θ range (°)	4.0–42°	4.0–43°
No. independent reflections	3420	3446
No. observed reflections [$F_o>4\sigma(F_o)$]	1080	1494
Solution and refinement		
Weighting scheme, w^{-1}	$\sigma^2(F)+0.2689F^2$	$\sigma^2(F)+0.0116F^2$
Final R; R' (observed data)	0.074; 0.077	0.066; 0.071
Largest peak on ΔF (e Å^{-3})	1.40	0.90

[a] Details in common: Mo Kα radiation ($\lambda=0.71073$ Å); $T=294$ K; highly oriented graphite-crystal monochromator; ω–2θ scans; ω scan speed 4.5–14.65° min^{-1}; scan range 0.60° + Kα separation; two standard reflections every 2 h; refinement by full-matrix least-squares minimizing $\Sigma w(|F_o|-|F_c|)^2$.

Table 2
Atomic coordinates ($\times 10^4$) with e.s.d values and equivalent isotropic displacement coefficients ($Å^2 \times 10^3$)

	1				2			
	x/a	*y/b*	*z/c*	U_{eq}	*x/a*	*y/b*	*z/c*	U_{eq}
Bi	116(1)	263(1)	3837(1)	43	678(1)	7688(1)	3218(1)	54
O(1a)	−893(16)	793(12)	4856(11)	77	846(5)	6773(6)	3996(6)	84
O(2a)	583(13)	1403(9)	3828(10)	42	827(5)	6749(5)	2475(5)	67
C(1a)	−2325(24)	1533(16)	5253(18)	60	1155(10)	5821(10)	4555(12)	94
C(2a)	−1324(25)	1378(19)	4878(19)	67	1055(7)	6145(7)	3900(9)	39
C(3a)	−829(35)	2004(22)	4507(25)	127	1213(7)	5873(8)	3290(12)	70
C(4a)	68(36)	1918(22)	3892(28)	110	1095(8)	6135(9)	2655(11)	74
C(5a)	457(28)	2619(20)	3643(21)	95	1197(9)	5766(10)	1967(10)	83
C(6a)	−2409(24)	975(18)	5938(17)	70	623(13)	5928(13)	5059(14)	175
C(7a)	−2297(32)	2253(21)	5651(25)	136	1837(13)	5962(13)	4750(15)	179
C(8a)	−3301(34)	1434(21)	4679(27)	127	1154(16)	5026(18)	4458(19)	247
C(9a)	−216(35)	3217(23)	3935(26)	141	1790(15)	6065(15)	1563(15)	197
C(10a)	1607(42)	2707(25)	4081(29)	173	633(13)	5816(13)	1502(14)	167
C(11a)	509(36)	2651(22)	2668(30)	153	1425(11)	5018(15)	2082(14)	154
O(1b)	1379(14)	443(10)	2856(11)	70	706(6)	8094(6)	2049(5)	72
O(2b)	−82(17)	−733(11)	2874(14)	82	728(5)	8907(6)	3208(6)	89
C(1b)	2505(22)	417(16)	1782(17)	57	1160(9)	8493(10)	1031(12)	85
C(2b)	1584(20)	87(13)	2182(16)	40	989(7)	8619(8)	1756(10)	58
C(3b)	1135(18)	−457(11)	1766(14)	20	1136(8)	9163(9)	2156(10)	66
C(4b)	284(25)	−786(17)	2144(20)	66	1011(8)	9344(10)	2806(11)	77
C(5b)	−174(18)	−1450(14)	1718(16)	24	1141(8)	10032(9)	3109(10)	77
C(6b)	3213(38)	−56(25)	1399(28)	161	716(14)	8049(15)	623(13)	174
C(7b)	1982(39)	839(26)	1039(30)	169	1870(14)	8270(15)	957(15)	187
C(8b)	3297(39)	922(26)	2278(29)	173	1125(18)	9198(19)	684(20)	259
C(9b)	300(36)	−1593(25)	923(28)	150	647(10)	10174(10)	3640(11)	115
C(10b)	−1407(38)	−1375(23)	1567(28)	155	1783(10)	9964(11)	3408(12)	112
C(11b)	108(40)	−2036(24)	2347(30)	158	1134(9)	10585(9)	2548(11)	94
O(1c)	−1408(15)	−396(10)	4151(11)	74	930(5)	8121(5)	4304(5)	61
O(2c)	−1101(16)	746(10)	2887(12)	75	1691(5)	7736(5)	3170(6)	59
C(1c)	−3023(25)	−899(17)	4189(19)	63	1446(10)	8500(10)	5249(12)	102
C(2c)	−2303(16)	−362(15)	3822(15)	14	1447(8)	8232(9)	4559(10)	72
C(3c)	−2580(28)	−73(20)	3119(25)	92	2050(7)	8101(8)	4284(9)	60
C(4c)	−1977(25)	422(19)	2652(19)	83	2088(7)	7876(7)	3595(9)	49
C(5c)	−2266(33)	497(22)	1679(24)	132	2755(9)	7802(10)	3325(11)	94
C(6c)	−2776(40)	−1602(28)	3929(31)	162	763(11)	8679(11)	5458(11)	125
C(7c)	−3092(31)	−872(20)	5194(25)	111	1683(12)	7937(14)	5730(14)	162
C(8c)	−4226(36)	−850(22)	3882(27)	151	1880(14)	9132(14)	5299(16)	188
C(9c)	−1655(31)	1118(21)	3534(24)	116	3267(18)	7887(17)	3887(20)	247
C(10c)	−1812(30)	−135(23)	1255(25)	200	2836(12)	7156(12)	2913(13)	151
C(11c)	−3501(31)	566(19)	1427(22)	122	2860(14)	8276(14)	2708(16)	189

O(1w)	4747(23)	−238(16)	1042(17)	166	51(15)	2945(14)	1784(17)	226					
O(2w)					0	2375(20)	2500	199					
O(3w)					0	3616(19)	2500	170					

Anisotropic displacement coefficients (Å^2×10^3)

	1						2					
	U_{11}	U_{22}	U_{33}	U_{12}	U_{13}	U_{23}	U_{11}	U_{22}	U_{33}	U_{12}	U_{13}	U_{23}
Bi	26(1)	54(2)	49(1)	−26(3)	−2(1)	0(3)	38(1)	49(1)	77(1)	0(1)	−2(1)	−2(1)

Table 3
Selected distances (mean e.s.d 0.02 Å for **1** and 0.01 Å for **2**) and angles (mean e.s.d 1° for **1** and 0.5° for **2**)

	1	2		1	2
Bi–O(1a)	2.36	2.38	O(1a)–Bi–O(2a)	75.4	77.4
Bi–O(2a)	2.30	2.36	O(1b)–Bi–O(2b)	74.0	70.2
Bi–O(1b)	2.32	2.41	O(1c)–Bi–O(2c)	82.0	78.4
Bi–O(2b)	2.47	2.39	O(2c)–Bi–O(1a)	84.7	85.0
Bi–O(1c)	2.38	2.34	O(2c)–Bi–O(2a)	75.4	82.9
Bi–O(2c)	2.26	2.13	O(2c)–Bi–O(1b)	86.8	85.4
Bi···Bi [a]	3.85	3.99	O(2c)–Bi–O(2b)	83.6	85.0
Bi···O(1b) [a]	3.03	3.05	O(2c)–Bi–O(1c)	82.0	78.4
O(1a)···O(2a)	2.81	2.96	O(2c)–Bi–Bi [a]	130.8	132.9
O(1b)···O(2b)	2.93	2.76	O(2c)–Bi–O(1b) [a]	154.5	158.4
O(1c)···O(2c)	3.04	2.83			

[a] At $-x$, $-y$, $1-z$ for **1**; at $-x$, y, $1/2-z$ for **2**.

bonding energy (BE) of the compound was analyzed in terms of Bi^{3+} and $acac^-$ fragment orbitals, applying Ziegler's generalized transition state method [10]:

$$BE=-[\Delta E_{es}+\Delta E_{Pauli}+\Delta E_{int}+\Delta E_{prep}]$$

where ΔE_{es} is the pure electrostatic interaction, ΔE_{Pauli} is the Pauli repulsion, ΔE_{int} the orbital interaction, and, finally, ΔE_{prep} is the deformation energy assumed by the fragments in order to form the complex. The first three terms form the so-called 'snapping energy' (BE_{snap}). To evaluate precisely fragment interaction energies, all the geometries were optimized at the non-relativistic (NR) local density approximation (LDA) level, using the Vosko–Wilk–Nusair formula [11]. Generalized gradient (GGA) corrections to the exchange-correlation potential, according to Becke [12] and Perdew [13], as well as quasi-relativistic (QR) scalar corrections, according to Snijders et al. [14] were included in the final calculations.

3. Results and discussion

3.1. Structure

The overall high thermal motion and the severe deterioration of the crystals during the data collection, as shown by the intensity decay (~20 and 40% for **1** and **2**, respectively) of the two standard reflections monitored at 2 h intervals, did not allow very accurate structural analysis of **1** and **2**. As a consequence, bond lengths and bond angles are not sufficiently precise to support arguments based on minor fluctuations in distances or angles. However, the models provide an adequate answer to binding/stereochemistry questions. Relevant data for the inner core are reported in Table 3. Both crystals are made of monomeric $Bi(dpm)_3$ units (Fig. 1) with the water molecules (one in **1** and three in **2**) trapped inside the lattice, with no significant interaction with the core of the complexes. Such water molecules most probably come from the benzene used for the recrystallization. The coordi-

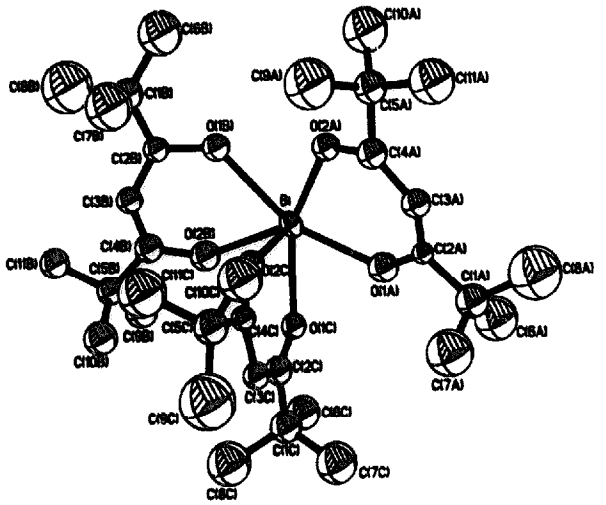

Fig. 1. ORTEP view of Bi(dpm)$_3$ in **2**.

nation sphere around bismuth is pentagonal pyramidal with the Bi atom below the basal plane (by 0.29 Å) and away from the apical O(2c) atom, such that the angles between the five basal donor atoms and the apical at Bi are all less than 90°. Structures **1** and **2** are roughly superimposable (Fig. 2), the weighted root mean square deviation, derived from the BMFIT program [15], being of 0.26 Å, when the fitting is performed using the 'inner core' atoms. It is noteworthy that a similar coordination around a Bi atom surrounded by six oxygenated donors has been only found in tris(ethylmaltolato)bismuth(III) [5]. In such complex there is a rather short Bi···O contact of 3.13 Å between two crystallographically related molecules to be compared with the 3.03 and 3.05 Å in **1** and **2**, respectively. Furthermore, in tris(ethylmaltolato)bismuth(III) the shortest Bi···Bi separation is 3.84 Å, while it is 3.85 and 3.99 Å in **1** and **2**, respectively. In addition, in complexes **1** and **2** the shortest Bi–O distance involves the apical oxygen (2.26 and 2.13 Å). Finally, the three water molecules in **2** site in the cylindrical cavity coaxial with the *b*-axis (Fig. 3) and the number of

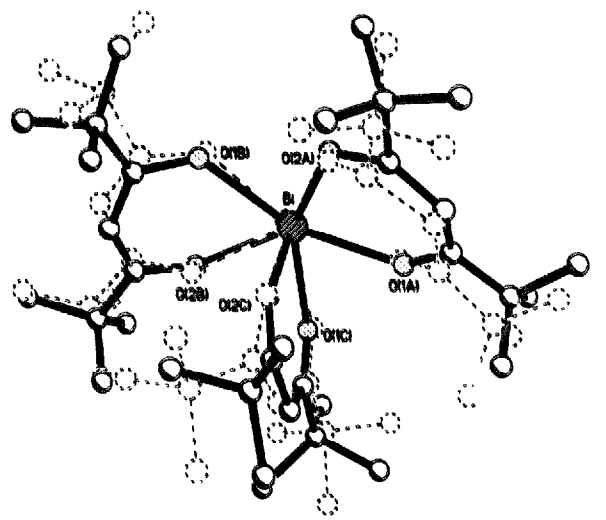

Fig. 2. Superimposition of structure **2** and **1** (- - -).

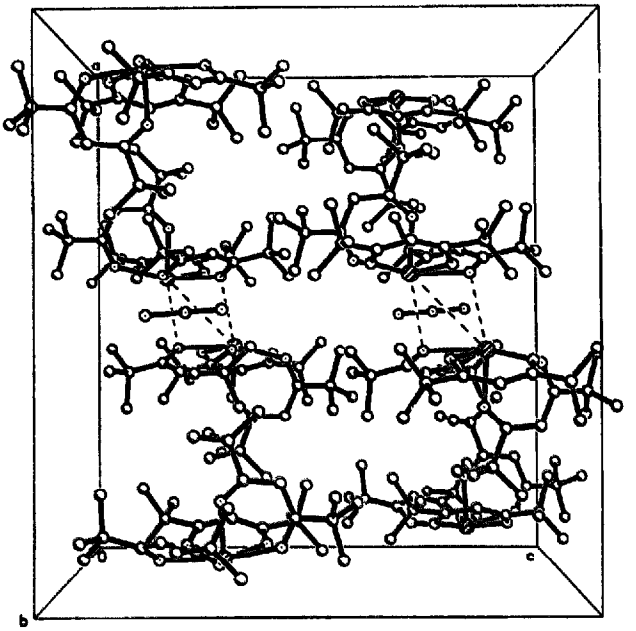

Fig. 3. Packing diagram of **2** viewed along the *y* axis. The dashed lines represent short intermolecular Bi···Bi and Bi···O(1b) contacts between related molecules.

water molecules in the unit cell of **2** was also confirmed by comparison of the unit volumes of **2** and **1**: 1000.7 versus 958.7 Å^3. The difference (42.0 Å^3) can be ascribed to two additional water molecules present in **2**, the water volume being 21.5 Å^3 [16].

3.2. C_s versus D_3: the stereoactivity of the Bi 6s lone pair

In order to clarify this issue we decided to compare the BE of the optimized C_s molecule with that pertinent to a hypothetical pseudo-octahedral D_3 structure (see Fig. 4), which is preferred in the case of no stereoactive lone pairs on the central metal ion. Both the geometries were optimized at the

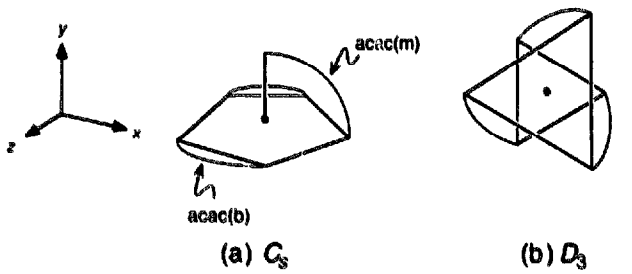

Fig. 4. Schematic views of (a) the C_s and (b) the D_3 structures. The axis framework adopted in the first case is also shown.

Table 4
Selected distances (Å) and angles (°) for Bi(acac)$_3$ (C_s) from NR-LDA optimizations

Bi–O(1a)	2.37	O(1a)–Bi–O(2a)	74.8
Bi–O(2a)	2.31	O(1c)–Bi–O(2c)	78.9
Bi–O(1c)	2.38	O(2c)–Bi–O(1a)	79.5
Bi–O(2c)	2.20	O(2c)–Bi–O(2a)	74.2

Table 5
Decomposition of the calculated interaction energies (eV) between Bi^{3+} and $acac^-$ ionic fragments according to the generalized transition state method for Bi(acac)$_3$ in the C_s and D_3 cases. The structures were optimized at the NR-LDA level

		ΔE_{es}	ΔE_{Pauli}	ΔE_{int}	BE_{snap}	ΔE_{prep}	BE
C_s	NR-LDA	−48.15	13.93	−16.03	−50.24	0.12	−50.12
	NR-GGA	−47.65	15.71	−15.66	−47.60	0.36	−47.24
	QR-GGA	−46.83	14.01	−14.98	−47.79	0.35	−47.44
D_3	NR-LDA	−46.38	10.77	−13.27	−49.15	0.09	−49.06
	NR-GGA	−46.23	11.96	−12.82	−47.09	0.12	−46.97
	QR-GGA	−45.56	10.30	−12.94	−48.20	0.12	−48.08

NR LDA level. In the C_s case, the main structural parameters (Table 4) are in good agreement with experiment (the acac fragments in the basal plane and the one in the *xy* mirror plane (see Fig. 4) are indicated as acac(b) and acac(m), respectively). Remarkably, the bonding distance of Bi with the axial oxygen of the ligand in the mirror position is significantly shorter than the others. This can be interpreted as first evidence of the repulsion between the lone pair and the basal oxygens.

From the Ziegler transition state analysis (Table 5) it appears that in both cases most part of the BE comes from the electrostatic term. Such a term is more favorable for the C_s structure, probably because of the closer metal–ligand

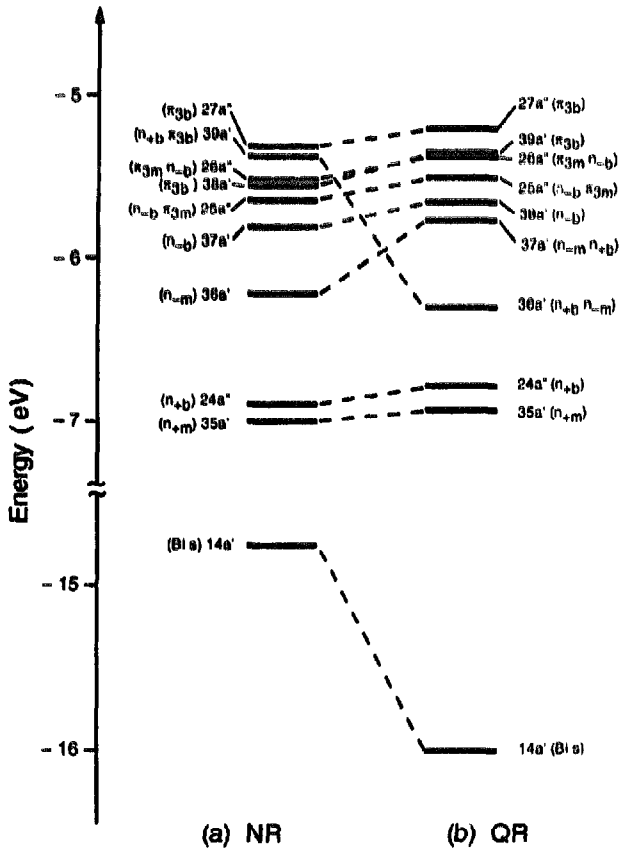

Fig. 5. One-electron energy levels of Bi(acac)$_3$ obtained from (a) NR and (b) QR calculations.

contact (the Bi–O distance is found to be 2.386 Å in the D_3 case, which is longer than any of the analogous distances in the C_s case). On the other hand, such a closer contact is offset by higher Pauli repulsions. We can also appreciate that GGA corrections cause a strong (~3 eV) BE reduction, according to the well-known overbinding tendency of the LDA. However, the most important issue is the comparison of the total BEs of the two structures: it turns out that, while in the NR approximation the C_s structure is slightly favored (~0.3 eV), when we turn on QR corrections the energy order is reversed, now favoring the D_3 structure. This can be understood in terms of the relativistic contraction of the Bi 6s orbital, which should lower its repulsion with the ligand combinations. We also have to point out that in the case of Bi(dpm)$_3$, the D_3 structure could be even more favored, because of the presence of more bulky ligands. So, why is Bi(dpm)$_3$ found in a C_s-like structure? In our calculations we mainly neglect two effects. The first is the dimeric interaction, whose existence is revealed by the Bi(dpm)$_3$ crystal structure. Though explorative calculations confirmed the presence of such interaction, a reliable estimate of its strength requires the full optimization of a large system with a low (C_1) symmetry, which is at present impossible with our computational resources. Another possibility is that the dimeric C_1 units allow a better crystal packing with respect to the D_3 units, minimizing intermolecular repulsions. Of course, these effects could play a role simultaneously. Anyway the key point is that the repulsion between the Bi s lone pair and the ligand electrons, though significant (see Section 3.3) is unable, by itself, to drive the geometry to the C_s pentagonal pyramidal structure. We believe that, in this regard, gas-phase structure determinations would be very interesting.

3.3. Electronic structure of the C_s monomer

Considerable insight into the bonding scheme of Bi(acac)$_3$ is obtained by making reference to the energy level scheme of Fig. 5, where the MOs' character according to the Evans notation [17] is also reported. We want to stress that the labelling is intended to give only the main contributions to each MO, since the low symmetry of the molecule causes some mixing among the various ligand combinations. We can appreciate that the s lone pair (MO 14a', see Fig. 6(a))

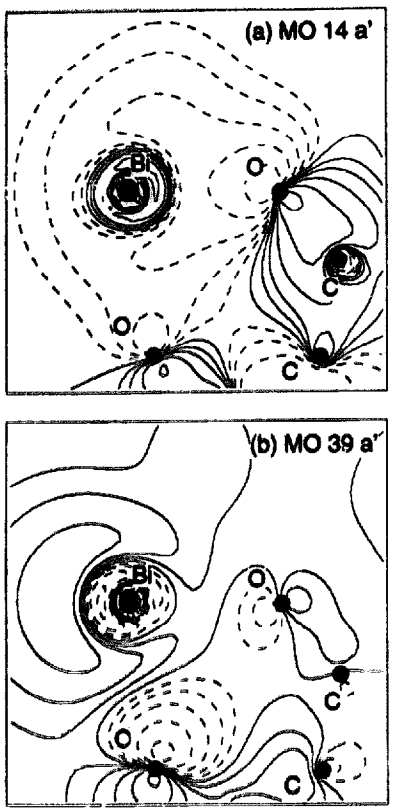

Fig. 6. Contour maps of (a) the 14a' and (b) the 39a' MOs, as obtained from NR calculations. The section is a 10×10 bohr^2 area in the xy mirror plane. Contour plot levels are 0, ± 0.00125, ± 0.025, ± 0.05, ± 0.1, ± 0.2 e$^{1/3}$ bohr$^{-3/3}$.

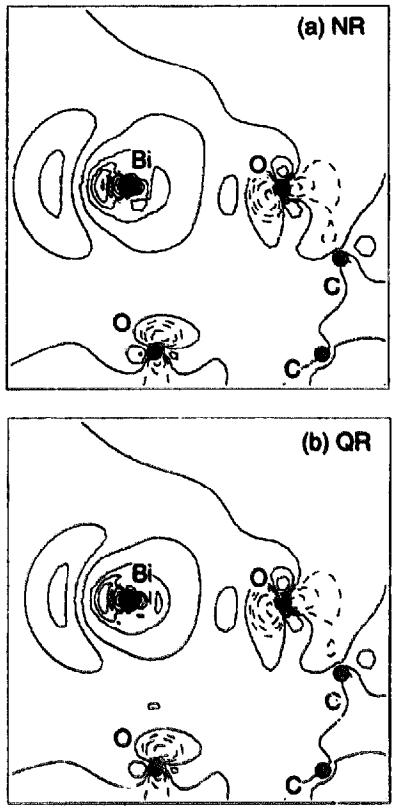

Fig. 7. Difference density maps (molecule fragments) for (a) NR and (b) QR cases. Section as in Fig. 6. Contour plot levels are 0, ± 0.00125, ± 0.025, ± 0.05, ± 0.1, ± 0.2 e bohr^{-3}.

is rather deep in energy. The energy sequence of the ligand-based combinations is typical of ionic β-diketonate compounds [17,18], confirming the generalized transition state analysis, with the anomaly of the n_{π}-based combination (MO 39 a', see Fig. 6(b)), which is pushed up in energy as a result of the repulsion with the Bi 6s lone pair. Maps reported in Fig. 6 show that such MO extends considerably below the basal plane along the x direction, while the true Bi s lone pair is almost spherical around the Bi center, contrary to the representation furnished by the VSEPR model. The difference density map reported in Fig. 7(a), obtained by subtracting the density of the Bi^{3+} and acac$^-$ fragments from the molecule density, show that, whatever the reason of the C_s structure, a large fraction of the molecule charge density is pushed away from the central atom along the x direction.

While GGA corrections introduce only minor modifications in the electronic structure (apart from an almost rigid slight shift of ~0.1 eV towards lower binding energies), quite interesting results are produced by the QR corrections (see Fig. 5). First of all, we observe a drastic stabilization of the 14a' MO, mainly composed of the Bi 6s AO (Fig. 8(a)). All the other levels are slightly destabilized, except the 39a' MO, which contains a large fraction of Bi s and p_x AOs. Such a level is stabilized by ~1 eV, at the same time strongly decreasing its p_x AO content, and corresponds to the MO 36a' (Fig. 8(b)) in the QR calculation. Such a behavior can be readily explained in terms of the reduced repulsion between the Bi 6s AOs and the ligand combinations: for this reason the need of localizing the s lone pair along the x axis, through s–p hybridization, is less important. This effect can be also appreciated by comparing the difference density plot reported in Fig. 6, but it results particularly evident from Fig. 9, where the difference between QR and NR charge densities is shown.

We turn now to examine the Mulliken [19] and the Hirshfeld [20] charges of the fragments reported in Table 6. Such data confirm once more the ionic nature of the Bi–acac bonds. Remarkably, upon including relativistic corrections, the charge of the Bi atom increases, but this effect is definitely stronger for the Mulliken analysis. We can explain such a difference by inspecting Table 7, where the Mulliken population of Bi is broken down in terms of AO contributions. A first point is that the s occupancy decreases by ~0.1 e which can be ascribed to the relativistic contraction of the 6s AO, now spanning a narrower space. On the other hand, the p_y and p_z occupancies are not affected at all, because the contraction of the Bi 6p AOs is negligible. Interestingly, this is not true for the p_x AO, whose population decreases of ~0.15 e. This fact provides quantitative support to the above-reported discussion regarding the s–p dehybridization.

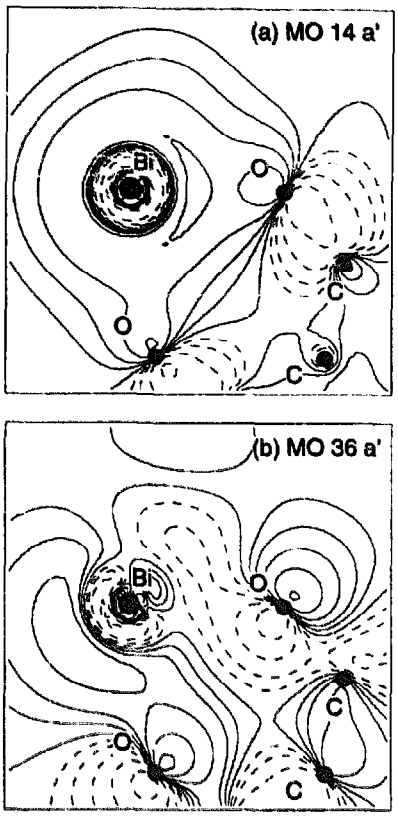

Fig. 8. Contour maps of (a) the 14a' and (b) the 36a' MOs, as obtained from QR calculations. Section and contour levels as in Fig. 6.

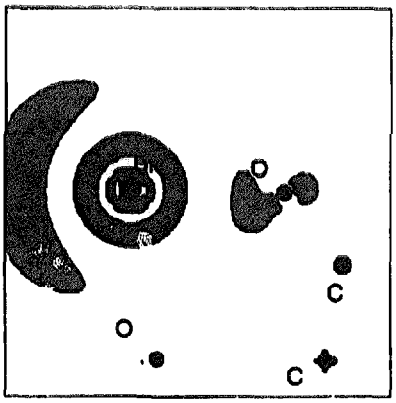

Fig. 9. Map representing the difference between QR and NR computed densities. Section as in Fig. 6. For clarity, only negative contours are shown (-0.025, -0.005, -0.010, -0.02 e bohr^{-3}), and all the areas where the difference is less than -0.025 e bohr^{-3} are shaded.

Table 6
Hirshfeld and Mulliken (in parentheses) charges of the fragments in $Bi(acac)_3$ (C_1)

	Bi	acac(b)	acac(m)
NR-LDA	2.18 (1.56)	−0.73	−0.66
NR-GGA	2.18 (1.61)	−0.75	−0.66
QR-GGA	2.26 (1.92)	−0.77	−0.77

Table 7
Mulliken populations of the Bi AOs in $Bi(acac)_3$ (C_1)

	s	p_x	p_y	p_z
NR-GGA	1.77	0.78	0.34	0.39
QR-GGA	1.65	0.66	0.34	0.40

4. Conclusions

We have synthesized $Bi(dpm)_3$ starting from $Bi(C_6H_5)_3$ and dpmH. Recrystallization in benzene yields crystals suitable for X-ray crystal structure determination. The ligands are coordinated around Bi in a pentagonal pyramidal fashion, with possible weak intermolecular bonds yielding dimeric units. DF calculations on the simpler $Bi(acac)_3$ complex show that the electrostatic interaction between the Bi^{3+} ion and the acac$^-$ ligands is the major contribution to the complex bonding energy. Although the theoretical geometry parameters for a C_1 $Bi(acac)_3$ molecule are very close to the experimental ones, the pseudo-octahedral D_3 isomer is found to be lower in energy. This means that the repulsion between the Bi s lone pair and the ligand combinations cannot be the only cause of the pentagonal pyramidal structure observed experimentally.

5. Supplementary material

Additional crystallographic data are available from G.B. on request.

Acknowledgements

The authors wish to thank the University of Perugia for access to their IBM SP2 system.

References

[1] R.K. Graselli and J.D. Burrington, Adv. Catal., 30 (1981) 133; H. Haeda, Y. Tamaka, M. Fukutoni and T. Asano, Jpn J. Appl. Phys., 27 (1988) L209; E. Moya, L. Contreras and C.T. Zaldo, J. Opt. Soc. Am. B, 5 (1988) 1737.
[2] A.P. Pisarevskii, L.I. Martynenko and N.G. Dzyubenko, Zh. Neorg. Khim., 37 (1991) 72 [English translation in Russ. J. Inorg. Chem., 37 (1992) 38]; M.-C. Massiani, R. Papiernik, L.G. Hubert-Pfalzgraf and J.-C. Daran, Polyhedron, 10 (1991) 437.
[3] E.O. Sidgwick and H.M. Powell, Proc. R. Soc. London, Ser. A, 176 (1954) 153; R.J. Gillespie and R.S. Nyholm, Q. Rev. Chem. Soc., 11 (1957) 339.
[4] G. Gottardi, Z. Kristallogr., 115 (1961) 451; M.C. Poore and D.R. Russel, J. Chem. Soc., Chem. Commun., (1971) 18; L.S. Lawton, C.J. Fuhrmeiser, R.G. Haas, C.S. Jarman, Jr. and F.G. Lohrmeyer, Inorg. Chem., 13 (1974) 135; C.L. Raston and A.H. White, J. Chem. Soc., Dalton Trans., (1976) 791; C.L. Raston, A.H. White and G. Winter, Aust. J. Chem., 31 (1978) 2207; B.F. Hoskins, E.R.T. Tiekink and G. Winter, Inorg. Chim. Acta, 81 (1984) L33; B.F. Hoskins,

E.R.T. Tiekink and G. Winter, Inorg. Chim. Acta, 99 (1985) 177; M.R. Snow and E.R.T. Tiekink, Aust. J. Chem., 40 (1987) 743.
[5] J. Burgess, J. Fawcett, S.A. Parsons and D.R. Russel, Acta Crystallogr., Sect. C, 50 (1994) 1911.
[6] A.F. Wells, Structural Inorganic Chemistry, Clarendon Press, Oxford, 5th edn., 1984.
[7] G.M. Sheldrick, SHELXTL-PLUS. An integrated system for solving, refining and displaying crystal structures from diffraction data, University of Göttingen, Germany, 1987.
[8] ADF 2.0.1, Department of Theoretical Chemistry, Vrije Universiteit, Amsterdam, 1995.
[9] D. Post and E.J. Baerends, J. Chem. Phys., 78 (1983) 5663; E.J. Baerends, D.E. Ellis and P. Ros, Chem. Phys., 2 (1988) 41; P.M. Boerrigter, G. te Velde and E.J. Baerends, Int. J. Quantum Chem., 33 (1988) 87; P.J. van der Hoek, A.W. Kleyn and E.J. Baerends, Commun. At. Mol. Phys., 23 (1989) 93; G. te Velde and E.J. Baerends, J. Comput. Chem., 99 (1992) 84.
[10] T. Ziegler and A. Rauk, Theor. Chim. Acta, 46 (1977) 1.
[11] S.J. Vosko, M. Wilk and M. Nusair, Can. J. Phys., 58 (1980) 1200.
[12] A. Becke, Can. J. Phys., 84 (1986) 4524; J. Chem. Phys., 88 (1988) 1053.
[13] J.P. Perdew, Phys. Rev. B, 33 (1986) 8822.
[14] J.G. Snijders and E.J. Baerends, Mol. Phys., 36 (1978) 1789; J.G. Snijders, E.J. Baerends and P. Ros, Mol. Phys., 38 (1979) 1909; T. Ziegler, V. Tschinke, E.J. Baerends, J.G. Snijders and W. Ravenek, J. Phys. Chem., 93 (1989) 3050.
[15] S.C. Nyburg, Acta Crystallogr., Sect. B, 30 (1974) 215.
[16] A. Immirzi and B. Perini, Acta Crystallogr., Sect. A, 33 (1977) 216.
[17] S. Evans, A. Hamnett, A.F. Orchard and D.R. Lloyd, Faraday Discuss. Chem. Soc., 54 (1972) 227.
[18] C. Furlani and C. Cauletti, Struct. Bonding (Berlin), 35 (1978) 119.
[19] R.S. Mulliken, J. Chem. Phys., 23 (1955) 1833.
[20] F.L. Hirshfeld, Theor. Chim. Acta, 44 (1977) 129; K.B. Wiberg and P.R. Rablen, J. Comput. Chem., 14 (1993) 1504.